Long-time behavior of the drag on a body in impulsive motion

By CHRISTOPHER J. LAWRENCE[1] AND RENWEI MEI[2]

[1] Department of Theoretical and Applied Mechanics, University of Illinois at Urbana–Champaign, Urbana, IL 61801, USA

[2] Department of Aerospace Engineering, Mechanics and Engineering Science, University of Florida, Gainesville, FL 32611, USA

Submitted to *Journal of Fluid Mechanics*, August 12, 1993.

We consider the response of the hydrodynamic force on a body in rectilinear motion to a change in the speed between two steady states, from U_1 to $U_2 \geq 0$. At large times, the laminar wake consists of two quasi-steady regions – the new wake and the old wake – connected by a transition zone that is convected downstream with the mean speed U_2. A global mass balance indicates the existence of a sink flow centered on the transition zone, and this is responsible for the leading order behavior of the unsteady force at long times. For the case of $U_1 \geq 0$, the force is shown to decay algebraically with the inverse square of time for any finite Reynolds number (Re), and this result is also shown to hold for non-rectilinear motions. For small Re, there is a near-cancellation in the case with $U_1 > 0$ which shifts the algebraic decay to higher order in Re than has been considered in small-Re asymptotic analyses. The case of reversed flow ($U_1 < 0$) and stopped flow ($U_2 = 0$) are treated separately, and it is shown that the transient force is dominated by the effects of the old wake, leading to a slower decay as the simple inverse of time. The force is determined by the far regions of the flow field and so the results are valid for any particle, bubble or drop and (in an average sense) for any Re, provided $\tau \gg \max\{\mathrm{Re}, \mathrm{Re}^{-1}\}$, where τ is the time made dimensionless with the convection timescale. The analytical results are compared to detailed numerical calculations for transient flow over spherical particles and bubbles and excellent agreement is obtained. These are believed to be the first calculations which fully resolve the transient far wake behind a bluff body at long times. The asymptotic result for the force is applied to determine that the approach to terminal velocity of a body in free fall is also as the inverse square of time.

1. Introduction

The drag on a body in transient motion has been of long-standing interest. It is relevant to such simple questions as the time-dependence of the velocity of a body in free fall, but it is particularly important in multiphase flows, where the transient hydrodynamic force plays a significant role in particle motions. Typical multiphase flows such as occur in spray combustion, fluidized beds, sedimentation, pneumatic transportation and slurry transportation are characterized by particle Reynolds numbers (Re_D based on relative velocity and particle diameter) in the range of unity to hundreds, while particle concentrations range from quite dilute to near close packing. Even for dilute suspensions whose particle-particle collisions may be neglected, the transient behavior of the fluid force on a particle in this range of Reynolds numbers is not known. Analytical approaches to the full time-dependent problem have been restricted to zero or small Reynolds numbers and to spherical or spheroidal bodies.

The long-time behavior of the hydrodynamic drag is of particular interest, since it determines the long-time statistics of random particle motions, including such important quantities as the particle diffusivity in turbulent flow (Reeks & McKee 1984, Mei, Adrian & Hanratty 1991) and velocity autocorrelations in Brownian motion (Hinch 1975). The classical approach using the Stokes equations yields a history force whose kernel decays as the inverse square root of time t (Basset 1888; see (1) below). This implies that a disturbance in velocity results in a decay of the transient force as $t^{-1/2}$. However, the low Reynolds number limit is known to be singular, and Sano (1981) has used matched asymptotic expansions to show that for an impulsively started motion at small Re_D the transient part of the force decays much more quickly, as the inverse square of time at long time. Mei and coworkers have used numerical solutions of the Navier-Stokes equation to determine the transient force at finite Re_D, and have obtained results which are consistent with the inverse square decay (Mei, Lawrence & Adrian 1991, Mei & Adrian 1992, Mei 1993a), as well as results which indicate a faster, possibly exponential, decay of the kernel at long times (Mei 1993b). Lovalenti & Brady (1993a, b, c) have considered quite general particle and drop motions at small Re_D; their analysis indicates that Sano's result is a rather special case and exponential decay may be expected in other situations. Rigorous analytical results are all restricted to zero or

asymptotically small Re_D and there remains considerable uncertainty as to which, if any, can be generalized to apply to finite Re_D [i.e. $\mathrm{Re}_D = O(1)$-$O(100)$]. In the present work, we seek to address the question: Is the long-time decay of the transient hydrodynamic force (and hence transient particle velocity) exponential or algebraic, and what is the correct exponent at finite Reynolds number?

Basset (1888) considered the hydrodynamic resistance to motion of a sphere of radius a with velocity $V(t)$ through fluid with viscosity μ and density ρ at zero Reynolds number, and obtained the result:

$$F(t) = -6\pi\mu a V(t) - 6\sqrt{\pi\mu\rho}a^2 \int_{-\infty}^{t} \dot{V}(s)\frac{ds}{\sqrt{t-s}} - \frac{2}{3}\pi\rho a^3 \dot{V}(t). \tag{1}$$

The first term is a quasi-steady viscous resistance, the third term is a purely inertial resistance known as the added-mass force, and the second term arises due to the diffusion of vorticity generated at the surface of the particle into the bulk of the fluid; it is variously known as the Basset force or history force. It is often convenient to consider a frame of reference in which the particle is fixed and the fluid moves with uniform velocity $U(t)$ in the far field. The frame of reference of the particle is non-inertial so there is an additional buoyancy-like term whose magnitude is given by the product of the acceleration and the mass of fluid displaced by the particle.

$$F(t) = 6\pi\mu a U(t) + 6\sqrt{\pi\mu\rho}a^2 \int_{-\infty}^{t} \dot{U}(s)\frac{ds}{\sqrt{t-s}} + 2\pi\rho a^3 \dot{U}(t). \tag{2}$$

For a step transition from U_1 to U_2 at time zero, the acceleration is simply a Dirac delta function and, for $t > 0$, (2) reduces to

$$F(t) = 6\pi\mu a U_2 + 6\sqrt{\pi\mu\rho}a^2 (U_2 - U_1)\, t^{-1/2}. \tag{3}$$

The linearized Navier-Stokes equations are somewhat tractable for spheroidal particles and semi-analytical expressions for the force have been obtained (Lawrence & Weinbaum 1988), while other geometries may be treated via boundary element methods (Pozrikidis 1989). A

Revised: August 12, 1993

generalization of (3) applies to the long-time behavior of the force on a particle of arbitrary geometry at zero Reynolds number (Williams 1966, Lawrence & Weinbaum 1988, Lovalenti & Brady 1993a):

$$F(t) \sim 3\pi\mu D\mathbf{A}\cdot U_2 + \frac{3}{2}\sqrt{\pi\mu\rho}D^2\mathbf{A}\cdot\mathbf{A}\cdot(U_2-U_1)\,t^{-1/2} \tag{4}$$

where $\mathbf{A}$ is the dimensionless resistance tensor for the body in steady Stokes flow, and D is the diameter of the body. The $t^{-1/2}$ decay at long times is characteristic of zero Reynolds number flow, but the limit is singular, due to the existence of an outer Oseen region where inertia is significant, so (3) and (4) are valid only for $\mathrm{Re}_2^{-1} \gg \tau \gg 1$, where $\tau = (U_2/a)\,t$ is the dimensionless time and $\mathrm{Re}_2 = U_2 D/\nu$. In the present work we consistently use the radius $a = D/2$ to form the dimensionless time, while the Reynolds number is based on diameter, except where explicitly indicated by the notation Re_a.

There has been some success in extending the above results to small Reynolds number through the use of matched asymptotic expansions. Sano (1981) considered the force on a sphere in an impulsively started uniform flow ($U_1 = 0$) at small Reynolds number, and obtained the asymptotic result:

$$F(\tau) = 1 + \frac{1}{3}\delta(\tau) + \frac{3}{8}\mathrm{Re}_a\left[\left(1+\frac{4}{T^2}\right)\mathrm{erf}\left(\frac{\sqrt{T}}{2}\right) + \frac{2}{\sqrt{\pi T}}\left(1-\frac{2}{T}\right)\mathrm{e}^{-T/4}\right] + \frac{9}{40}\mathrm{Re}_a^2\log\mathrm{Re}_a + O(\mathrm{Re}_a^2) \tag{5}$$

in which the force has been made dimensionless with the steady Stokes drag $6\pi\mu a U_2$, the Reynolds number is $\mathrm{Re}_a = U_2 a/\nu$, and $T = \mathrm{Re}_a\tau = (U_2^2/\nu)\,t$. The long-time behavior is characterized by an inverse square decay:

$$F(T) \sim \left(1 + \frac{3}{8}\mathrm{Re}_a + \frac{9}{40}\mathrm{Re}_a^2\log\mathrm{Re}_a\right) + \frac{3}{2}\mathrm{Re}_a T^{-2}. \tag{6}$$

Recent work by Lovalenti & Brady (1993a) has made use of a general reciprocal theorem to obtain the force on a spherical particle in arbitrary motion at small Reynolds number:

$$F(\tau) \sim U(\tau) + \frac{1}{9}\mathrm{Re}_a \dot{U}(\tau) + \frac{2}{9}\mathrm{Re}_a \dot{u}(\tau) + \frac{1}{8}\mathrm{Re}_a^{1/2}\pi^{-1/2}\int_{-\infty}^{\tau}\left[2F_S^{\parallel}(\tau) - \frac{3}{A^2}\left(\frac{\sqrt{\pi}}{2A}\mathrm{erf}(A) - e^{-A^2}\right)F_S^{\parallel}(s)\right.$$

$$\left. + 2F_S^{\perp}(\tau) - 3\left\{e^{-A^2} - \frac{1}{2A^2}\left(\frac{\sqrt{\pi}}{2A}\mathrm{erf}(A) - e^{-A^2}\right)\right\}F_S^{\perp}(s)\right]\frac{2ds}{(\tau - s)^{3/2}} + o(\mathrm{Re}_a) \tag{7}$$

where $\boldsymbol{U}(t) = \boldsymbol{u}(t) - \boldsymbol{V}(t)$ is the difference between the velocity of the fluid in the neighborhood of the particle $\boldsymbol{u}(t)$ and the particle velocity $\boldsymbol{V}(t)$, A relates to the magnitude of the relative displacement between times s and τ,

$$A(\tau, s) = |\boldsymbol{A}(\tau, s)| = \frac{1}{2}\mathrm{Re}_a^{1/2}(\tau - s)^{-1/2}\left|\int_s^{\tau}\boldsymbol{U}(s')ds'\right| \tag{8}$$

and $\boldsymbol{F}_S^{\parallel}(s)$, $\boldsymbol{F}_S^{\perp}(s)$ are the components of the pseudo-steady Stokes drag (with our scaling simply the velocity) at time s, respectively parallel and perpendicular to the displacement vector $\boldsymbol{A}(\tau, s)$.

A long-time representation for the force on an arbitrary particle at small Reynolds number was also obtained. This is somewhat complicated, but the specialization to a step-change in rectilinear velocity from $U_1 = \alpha_{12}U_2$ to U_2 is of particular interest. The $O(\mathrm{Re}_a)$ correction to the steady Stokes result for the component of the force parallel to the flow is given as:

$$F_1(T) = \frac{3}{8}\mathrm{Re}_a\phi_0^2 f(T) \tag{9}$$

where ϕ_0 is the parallel component of the dimensionless Stokes resistance tensor. In the special case of an impulsive start from rest, $f(T)$ takes the identical form to Sano's result (5) for all time. In other cases, the long-time behavior is given by:

Revised: August 12, 1993

$$f(T) \sim \begin{cases} 1 + \dfrac{4}{(1-\alpha_{12})^2} T^{-2} e^{-\alpha_{12}(1-\alpha_{12})T}, & 0 \le \alpha_{12} < \dfrac{1}{2} \\ 1 + 8T^{-2} e^{-T/4}, & \alpha_{12} = \dfrac{1}{2} \\ 1 + \dfrac{32}{\sqrt{\pi}} \dfrac{1-\alpha_{12}}{2\alpha_{12}-1} T^{-5/2} e^{-T/4}, & \alpha_{12} > \dfrac{1}{2} \\ -2T^{-1} + \dfrac{4}{\sqrt{\pi}} T^{-3/2}, & \alpha_{12} \to \infty \end{cases} \tag{10}$$

The final case corresponds to suddenly stopped motion ($U_2 = 0$), so the Reynolds number and timescale are necessarily based on U_1. An interesting feature of Lovalenti & Brady's work is the singular difference between the case where either U_1 or U_2 is zero and the case of a transition between two finite speeds. In the former case, the force decays algebraically in time (as T^{-2} or T^{-1}), while in the latter case, the force decays exponentially in time.

The available evidence concerning the long-time decay of the force at finite Reynolds number [$\mathrm{Re}_D = O(1)$-$O(100)$] is somewhat mixed. The older literature contains a number of different *ad hoc* approaches (see Clift, Grace & Weber 1978). Recent numerical work has focussed on three different canonical forms of $U(t)$ for flow past a sphere: a small fluctuation about a steady flow (Mei, Lawrence & Adrian 1991, Mei & Adrian 1992), a large amplitude oscillation with zero mean (Mei 1993a), and an impulsive change in velocity from $U_1 \ge 0$ to $U_2 > 0$ (Mei 1993b).

Mei & Adrian (1992) proposed the following decomposition for the time-dependent force on a rigid sphere at finite Reynolds number

$$F(t) = F_{\mathrm{QS}}(t) + F_H(t) + F_{\mathrm{AM}}(t) + F_{\mathrm{FS}}(t) \tag{11}$$

with contributions from the quasi-steady drag

$$F_{\mathrm{QS}}(t) = 6\pi\mu a U(t) \phi(\mathrm{Re}_D) \tag{12}$$

the history force

$$F_H(t) = 6\pi\mu a \int_{-\infty}^{t} K(t, s; \mathrm{Re}_D)\dot{U}(s)ds \tag{13}$$

the added mass force

$$F_{\mathrm{AM}}(t) = \frac{2}{3}\pi\rho a^3 \dot{U}(t) \tag{14}$$

and the "buoyancy" force due to the acceleration of the free stream:

$$F_{\mathrm{FS}}(t) = \frac{4}{3}\pi\rho a^3 \dot{u}(t). \tag{15}$$

The Reynolds number $\mathrm{Re}_D(t) = 2aU(t)/\nu$ is based on the diameter of the sphere and the instantaneous relative velocity, and the factor $\phi(\mathrm{Re}_D)$ accounts for the deviation from the Stokesian drag law. Clift, Grace & Weber (1978) have collected several different correlations for ϕ of which the best are:

$$\phi(\mathrm{Re}_D) = \begin{cases} 1 + \dfrac{3}{16}\mathrm{Re}_D & 0 < \mathrm{Re}_D < 0.01 \\ 1 + 0.1315\mathrm{Re}_D^{0.82 - 0.05w} & 0.01 < \mathrm{Re}_D < 20 \\ 1 + 0.1935\mathrm{Re}_D^{0.6305} & 20 < \mathrm{Re}_D < 260 \end{cases} \tag{16}$$

with $w = \log_{10}\mathrm{Re}_D$. Mei & Adrian (1992) proposed the following approximation for the history force kernel based on the numerical results of Mei, Lawrence & Adrian (1991) for small oscillations about a mean flow, and an asymptotic analysis of the same flow at small Reynolds number

$$K(t, s) \approx \left\{ \left[\frac{\pi\nu}{a^2}(t-s) \right]^{1/4} + \left[\frac{\pi}{2a\nu} \left(\frac{U(s)}{f_H} \right)^3 (t-s)^2 \right]^{1/2} \right\}^{-2} \tag{17}$$

with $f_H(\mathrm{Re}_D) = 0.75 + 0.105\mathrm{Re}_D(s)$. The $t^{-1/2}$ behavior for small times was shown to be asymptotically correct, but the t^{-2} decay at long times is an artifact of the interpolation procedure (Mei 1993b, Lovalenti & Brady 1993b). It is consistent with Sano's (1981) result,

Revised: August 12, 1993

but not with the more recent results of Lovalenti & Brady (1993a, b), which indicate exponential decay of the kernel at long times, at least for small Reynolds number.

Mei (1993b) has computed the force for an impulsively started flow or a step change in velocity, in which case $\dot{U}$ reduces to a delta function, so the kernel of the history force (13) can be found directly by subtracting the quasi-steady component (12) from the total force (11). The detailed numerical result is reasonably consistent with the kernel obtained from the linearized problem given in (17), although the very long-time behavior of the computed force was somewhat uncertain; it could be interpreted alternatively as an algebraic decay somewhat faster than the inverse square of time, or as a slow exponential decay. In the case of a large amplitude oscillatory flow with zero mean (Mei, 1993a), the approximation (17) gave very good results for the history force at moderate and high frequencies with finite Re_D. At low frequencies, however, (17) gives only the correct order of magnitude of the oscillatory history force, while Basset's expression (1) leads to a substantial over-prediction of the history force at finite Reynolds number. Thus, the long-time behavior of $K(t, s)$ is not known for the most general case.

The objective of the present work is to contribute to a resolution of the questions posed above by deriving general results for the long-time behavior of the drag on a body which undergoes a transition in velocity. The approach follows closely the analysis of the steady wake elucidated by Batchelor (1967). The hydrodynamic force is determined in terms of the gross features of the flow field through the application of global conservation principles, without the need for a detailed analysis of the flow in the vicinity of the body. The features of the flow field are discussed in Section 2, new asymptotic results for the force are derived in Section 3, and these results are compared with detailed numerical solutions for the force. The principal asymptotic result confirms t^{-2} decay of the force for both unidirectional and non-parallel changes in the velocity; the cases of reversed and suddenly stopped flow are treated separately, and the force is shown to decay as t^{-1}. In Section 4 the asymptotic results are applied to determine the approach to terminal velocity of a body in free fall which is also found to follow t^{-2} decay. The new results are summarized and discussed in Section 5.

As this work was completed, the authors became aware of the Appendix by E. J. Hinch added to Lovalenti & Brady (1993a). The analytical results for impulsively started and stopped flow given below are essentially identical to those given by Hinch, although other results are different.

2. Features of the flow field

The velocity field for steady flow past a body is dominated at large range by three principal features: the uniform oncoming velocity U_1, the steady wake of the body which directs a net flow Q_1 towards the body, and a consequent simple source flow of strength Q_1 centered on the body. These features are illustrated in Figure 1. A global accounting of conservation of mass and momentum for the control volume shown dashed in Figure 1 leads to a very simple relationship between the force on the body and the wake flux:

$$F_1 = \rho U_1 Q_1 \tag{18}$$

When the flow speed is changed to a new value U_2, the old wake will be convected downstream, but will remain steady relative to a frame moving with speed $(U_2 - U_1)$, and a new wake will be generated in the region immediately downstream of the sphere. This configuration is illustrated in Figure 2. After a sufficiently long time has elapsed, the new wake will become quasi-steady in the region $0 < x < U_2 t$, and the old wake will persist in the region $x > U_2 t$. There will be a roughly spherical transition zone (labelled T. Z. in Figure 2), which grows as $\sqrt{\nu t}$ and moves downstream with speed U_2, in which the two wakes are joined smoothly. The principal balance in the two wake regions is between advection and cross stream diffusion of vorticity; these mechanisms are supplemented by streamwise diffusion in the transition zone.

The volume flux in the old wake persists at the old value Q_1, while that in the new wake will be Q_2; both fluxes may be found from the corresponding steady drag:

$$Q_i = \frac{F_i}{\rho U_i} \qquad i = 1, 2 \tag{19}$$

Revised: August 12, 1993

The two fluxes will not in general be equal, so the mass balance must be completed by a sink flow centered on the transition zone at $x = U_2 t$ of strength $Q_2 - Q_1$ (or a source if $Q_2 < Q_1$). The large-scale features of the flow field at long time may thus be represented as in Figure 2. Of particular significance is the absence of nonlinearity in the far field. The principal components of the flow all derive from linear theory and so may be superposed without direct interaction.

In the special case of start-up from rest, the old wake is absent and $Q_1 = 0$. The source near the body and the sink in the transition zone are of equal strength Q_2, forming a "dipole" which is gradually stretched out. At large times, the sink flow is "left behind" at the starting point, while the body carries the source flow with it. The distance between the source and sink is $U_2 t$, and at distances much greater than $U_2 t$ the flow field is simply given by a potential dipole of strength $Q_2 U_2 t = (F_2/\rho)\, t$.

3. The unsteady force on the body

3.1 Analysis for an arbitrary body

The unsteady force on the body may be obtained using a global momentum balance as in the steady state, with the additional feature that the unsteadiness of the flow must be explicitly accounted for by an integration of the fluid acceleration over the whole control volume. A detailed description of the leading order asymptotic flow field in the new wake, the old wake and the transition zone will be presented elsewhere (Mei & Lawrence 1993). For our present purpose, it is sufficient to know that the integration over a large control volume of size much greater than $U_2 t$ as shown in Figure 2 leads to the quasi steady result $F = F_2 = \rho U_2 Q_2$.

We are left with the conclusion that unsteady contributions to the force must derive from higher order contributions to the wake or transition zone flow fields. A higher order asymptotic analysis is quite tedious, but may be circumvented for the present purposes by consideration of the smaller control volume of size much greater than the body, but much less than $U_2 t$, shown in Figure 2. The flow field in this smaller volume is quasi-steady, but the mean flow is

increased somewhat above U_2 due to the influence of the sink flow centered on the transition zone

$$U \sim U_2 + \frac{Q_2 - Q_1}{4\pi (U_2 t)^2} = U_2 (1 + \lambda) \tag{20}$$

The force may then be obtained as the quasi-steady force corresponding to the "local" speed U.

It is convenient to represent the quasi-steady force in dimensionless form, based on the low Reynolds number drag, as in (12) and (16) above

$$F_{QS} = 3\pi\mu D U \phi(\mathrm{Re}_D). \tag{21}$$

We then obtain the wake flux from (19) as

$$Q_i = 3\pi\nu D \phi_i \tag{22}$$

where $\phi_i = \phi(\mathrm{Re}_i)$ with $\mathrm{Re}_i = U_i D/\nu$. The dimensionless local velocity increment due to the sink is then given by

$$\lambda \sim \frac{Q_2 - Q_1}{4\pi U_2^3 t^2} = \frac{3}{\mathrm{Re}_2} (\phi_2 - \phi_1) \tau^{-2} \tag{23}$$

in which $\tau = tU_2/a$ is the dimensionless time.

We decompose the force into steady and transient parts:

$$F(\tau) = 3\pi\mu D U_2 (\phi_2 + \phi_H(\tau)) \tag{24}$$

in which the transient part is found from (21) as

$$\begin{aligned} \phi_H &= (1+\lambda)\,\phi((1+\lambda)\mathrm{Re}_2) - \phi_2 \\ &\sim \lambda (\phi_2 + \mathrm{Re}_2 \phi'_2), \qquad \lambda \ll 1 \end{aligned} \tag{25}$$

where ϕ' is the derivative of ϕ with respect to Re. Finally we have the principal result of this paper:

Revised: August 12, 1993

$$\phi_H \sim \frac{3}{\mathrm{Re}_2}(\phi_2 + \mathrm{Re}_2\phi'_2)(\phi_2 - \phi_1)\tau^{-2} \tag{26}$$

where we note that ϕ_1 is taken to be zero for the case of start-up from rest ($U_1 = 0$). The result (26) indicates that the transient force should decay to the steady drag as the inverse square of time, $\phi_H \propto \tau^{-2}$ for all finite Reynolds number, whether the initial velocity is zero or not.

For very small Reynolds numbers, the quantity ϕ is linear in Re_D, $\phi \sim \phi_0 + \mathrm{Re}_D\phi'_0$, so there is a near cancellation due to $\phi_2 - \phi_1$ in (26). For a spherical particle, we may use the asymptotic result of (16) for ϕ, so that if the initial velocity is non-zero (26) simplifies to give

$$\phi_H \sim \frac{9}{16}(1-\alpha_{12})\tau^{-2} = \frac{9}{16}\mathrm{Re}_a^2(1-\alpha_{12})T^{-2} \tag{27}$$

where $T = \mathrm{Re}_a\tau = (U_2^2/\nu)t$ and $\alpha_{12} = |U_1/U_2|$ is the ratio of the initial to the final velocity. In the case of flow started from rest, we use the value $\phi_1 = 0$, so there is no cancellation in (26). For the case of a spherical particle at small Reynolds number, we use $\phi_2 \sim \phi_0 = 1$ and recover the long-time form of Sano's (1981) result:

$$\phi_H \sim \frac{3}{\mathrm{Re}_2}\tau^{-2} = \frac{3}{2}\mathrm{Re}_a T^{-2}. \tag{28}$$

In either case (27) or (28), the decay of the force is as the inverse square of time, but the coefficient changes from $O(\mathrm{Re}_a)$ for impulsively started flow to $O(\mathrm{Re}_a^2)$ for non-zero initial velocity. The asymptotic analysis of Lovalenti & Brady (1993a, b) is accurate only to $O(\mathrm{Re}_a)$ and so is unable to capture the correct long-time behavior exhibited in (27).

The case of non-parallel flow may also be addressed within the present framework. If $\boldsymbol{U}_1$ and $\boldsymbol{U}_2$ are non-parallel vectors, the flow field sketched in Figure 2 would be changed in that the portion of the old wake would be rotated about an axis in the transition zone to align with $\boldsymbol{U}_1$. The details of the flow in the transition zone would change considerably, but the strength of the sink would still be $Q_2 - Q_1$. The argument leading to the result (26) for the force would not be affected, and so we would obtain exactly the same result as above, with ϕ_i representing

the magnitude of the respective steady forces. The direction of the force remains parallel to U_2.

In the case of a complete flow reversal ($U_1 < 0$), the old wake will be upstream of the particle, and will be swept back towards the body. The flow speed near the body is increased due to the flux in the old wake, by an amount which scales with $1/t$ at long times. From Batchelor (1967) we may obtain the velocity in the old wake as:

$$U \sim U_2 + \frac{Q_1 |U_1|}{4\pi\nu x} \tag{29}$$

where x is the distance from the "origin" of the old wake which is swept downstream with speed $(U_2 - U_1)$, i.e. $x = (U_2 - U_1)\, t$. In the notation of (25), λ is given by:

$$\lambda \sim \frac{\alpha_{12} Q_1}{4\pi\nu (U_2 - U_1) t} = \frac{3}{2} \frac{\alpha_{12}\phi_1}{(1+\alpha_{12})\tau}. \tag{30}$$

We may also account directly for the effect of the sink at $x = U_2 t$ to give

$$\lambda \sim \frac{3}{2} \frac{\alpha_{12}\phi_1}{(1+\alpha_{12})\tau} + 3 \frac{\phi_2 - \phi_1}{\mathrm{Re}_2 \tau^2} \tag{31}$$

However, in practise, the sink term will never be very important: For an exact reversal of the flow ($U_1 = -U_2$), it will be zero, for large Reynolds number it will be small because of the factor Re_2^{-1}, and for small Reynolds number, there is a near cancellation in the factor $(\phi_2 - \phi_1)$. So we use the simpler form

$$\phi_H \sim \frac{3}{2} (\phi_2 + \mathrm{Re}_2 \phi'_2) \frac{\alpha_{12}}{1+\alpha_{12}} \phi_1 \tau^{-1}. \tag{32}$$

The different nature of the force for reversed flow may be partly responsible for the relatively poor performance of Mei & Adrian's (1992) approximation for the history force in the case of large amplitude oscillations at low frequency (Mei 1993a). In the general context of multiphase flows, particle trajectories are not likely to be rectilinear, so the probability of instantaneous flow reversals is small, and the result (26) may be more useful than (32).

Revised: August 12, 1993

The case in which the flow is suddenly brought to rest ($U_2 = 0$) is somewhat different, since the new wake is absent, and the transition zone grows around the body. We may expect that the force will be dominated by the effects of the old wake, as in reversed flow, but note certain differences. The velocity in the part of the *old wake* adjacent to the transition zone will be simply

$$U \sim \frac{Q_1}{4\pi\nu t} \tag{33}$$

while the velocity on the opposite side of the transition zone will be zero. In general, the transition zone is merely a diffusive connection between the old wake and the new wake, and the velocity at its center is precisely the mean of the wake velocities on either side (Mei & Lawrence 1993). In the present case, the body sits in the center of the transition zone, so it sees an ambient velocity given by one half of (33). Thus the force on the body is given by

$$\phi_H \sim \frac{3}{4}\phi_0\phi_1\tau^{-1} \tag{34}$$

where ϕ_0 gives the drag on the body at zero Reynolds number. In this case, there is no steady contribution to the drag, so (34) gives the leading order behavior. For small Reynolds number flow, (34) reduces to the result of Lovalenti & Brady (1993a),

$$\phi_H \sim \frac{3}{4}\phi_0^2\tau^{-1} = \frac{3}{8}\phi_0^2 \mathrm{Re}_a(2T^{-1}) . \tag{35}$$

3.2 Computational results for flow past a sphere

The long-time asymptotic results (26), (32), (34) derived above may be compared with detailed numerical solutions of the full Navier-Stokes equations for flow past a sphere (Mei & Lawrence, 1993). Extreme caution was required in the discretization of the system in order to resolve the features of the flow field shown in Figure 2, and to retain accuracy in the computation of the force up to very long times. To the best of our knowledge these are the first fully resolved computations of a strongly transient flow past a bluff body at long times.

Figure 3 shows a comparison of the numerical and long-time asymptotic result (26) for the transient component of the force ϕ_H due to impulsively started flow ($\alpha_{12} = 0$). For each Reynolds number, the history force initially decays as $\tau^{-1/2}$ given by Basset's result, and gradually changes to the asymptotic τ^{-2} decay at large times. The long-time asymptotic result is formally valid for $\tau \gg \max\{\mathrm{Re}, 1/\mathrm{Re}\}$, and we see that this requirement is in general necessary for the asymptotic result to be accurate. Sano's (1981) small Re asymptotic result is excellent for the smallest Reynolds number shown (Re = 0.1), and remains useful up to Re = 1. The approximation given by Mei & Adrian (1992) is qualitatively correct in each case, although it does not give the correct coefficient of the τ^{-2} decay.

Figure 4 shows the results for a step change with different values of α_{12} and Re. Actually shown is the history force kernel defined by (11) and (13) or, more simply,

$$\phi_H = (1-\alpha_{12})\,K(\tau)\,. \tag{36}$$

Figure 4(a)-(d) are for an increase in velocity with $\alpha_{12} < 1$, while Figure 4(e) is for a decrease in velocity with $\alpha_{12} = 4$. The qualitative features of the curves are all the same, and similar to those of Figure 3; there is a transition from Basset's $\tau^{-1/2}$ decay at small times to the new τ^{-2} decay at long times, with a slight bulge in the force before it falls off to the long-time asymptote. Again, we see that Mei & Adrian's (1992) approximation performs quite well in each case, with a substantial quantitative error only when the history force itself is quite small.

The case of small Reynolds number ($\mathrm{Re}_1 = 0.1$, $\mathrm{Re}_2 = 0.3$) shown in Figure 4(a) is of particular interest. We see that Lovalenti & Brady's (1993a) solution is qualitatively correct only up to $\tau \sim 100$. The long time τ^{-2} decay of the present theory is strongly evident in the numerical result, although there is a short period around $\tau \sim 100$ when the history force decreases rapidly, and this is clearly related to the exponential decay of Lovalenti & Brady's (1993a) result. Since the $O(\mathrm{Re})$ contribution decays exponentially, it is swamped by the $O(\mathrm{Re}^2)$ contribution at large times and, as with Basset's (1888) solution, Lovalenti & Brady's (1993a) solution ceases to be asymptotically correct when $\tau = O(\mathrm{Re}^{-1})$.

Revised: August 12, 1993

The numerical results presented in both Figure 3 and Figure 4 are not quite perfect. Since no special treatment of the initial Stokes boundary layer was made, there is some oscillation evident at small times, but this quickly dies away, and does not affect the history force at longer times, which is dictated by the strength of the sink in the transition zone. At very long times, the resolution of the transition zone is not sufficient, so none of the numerical results are accurate for a dimensionless time greater than about 300.

The contrast between the cases $U_1 > 0$ and $U_1 = 0$ is even more apparent in Figure 5(a), where we plot $|C|$, the magnitude of the coefficient of the inverse square decay $\phi_H \sim C\tau^{-2}$, as a function of Re_D for different values of α_{12}. The coefficients vary very little over the range of Reynolds numbers from 0 to 250, with the notable exception of the curve for $\alpha_{12} = 0$, which is strongly singular for small Re_D. The curves for $\alpha_{12} > 0$ are paired at small Reynolds number according to the value of $|1 - \alpha_{12}|$ and it is notable that the paired curves remain close even for relatively large values of Re_D. The strong overall similarity between the curves for $\alpha_{12} > 0$ in Figure 5(a) is brought out further in Figure 5(b) where we plot the coefficient from the history force kernel $C/(1 - \alpha_{12})$. This quantity varies very little over the range $0.1 < \alpha_{12} < 4$ and $0 < \mathrm{Re}_D < 10^2$, showing that the long-time response of the force is almost linear with respect to the two velocities for this range of parameters, and the history force may be approximated by the simpler formula $\phi_H \sim 0.1\,(1 - \alpha_{12})\,\tau^{-2}$. Figure 5 was prepared using the approximate form (16) of the steady drag law for a sphere; this results in discontinuities as Re_1 and Re_2 cross the connecting values of 0.01 and 20.

Next, we examine the results for flow reversal and stoppage. Figure 6 shows the transient part of the drag for completely reversed flow ($\alpha_{12} = 1$) for a moderate Reynolds number (Re=10) – we see that equation (32) gives very good agreement at long times. Figure 7 shows the total force on a sphere in a flow which is suddenly brought to rest (34). In this case, the very strong oscillation in the initial transient is a direct result of incorrect treatment of the initial conditions, but does not affect the long-term result. In fact, the computations for flow reversal and stoppage are easier at large times than the step-change cases, because the τ^{-1} decay leads to a larger magnitude of ϕ_H and numerical errors are less significant.

Finally, we compare the long-time asymptotic result (26) with numerical results for flow over a spherical bubble (Mei, Klausner and Lawrence, 1993). The computations are very similar except that the no-slip condition is replaced by a zero shear boundary condition for the bubble. Although the wake behind a bubble is smaller and weaker than for a rigid particle, the general features depicted in Figure 2 are the same. Hence (26) is expected to be valid for the bubble. An approximate expression for $\phi(\mathrm{Re})$ has been proposed (Mei, Klausner and Lawrence, 1993) as:

$$\phi_{\text{bubble}} = \frac{2}{3} + \left[\frac{12}{\mathrm{Re}_D} + 0.75\left(1 + \frac{3.315}{\mathrm{Re}_D^{1/2}}\right)\right]^{-1} \tag{37}$$

which reduces to $\phi_{\text{bubble}} = 2/3 + 12/\mathrm{Re}_D$ for small Re_D and to $\phi_{\text{bubble}} = 2\,(1 - 2.21/\mathrm{Re}_D^{1/2})$ for large Re_D. Equation (37) also compares very well with the numerical results for finite Re_D (Mei & Klausner, 1992).

Based on (26) and (37), the long-time transient force for impulsively started flows with $\mathrm{Re}_D = 5$ and 40 are $1.064/t^2$ and $0.120/t^2$ respectively. Figure 8 shows that the finite difference results agree quite well with the long-time asymptotic results. For small t, the history force asymptotes to a constant instead of the Basset $t^{-1/2}$ behavior due to the mobility of the surface. It is noted that the transient force is much smaller for a bubble than for a solid sphere at a given Re_D, because of the much weaker wake. Hence it is more difficult to accurately capture the effect of the sink in the transition zone for the case of a bubble and the numerical error may be larger.

4. A body in free fall

The new results may be used to obtain long-time solutions to simple problems such as the approach to terminal velocity of a body in free fall. If a body of mass m is released from rest at $t = 0$, its velocity V will satisfy the equation of motion

$$m\dot{V} = F(t) + (m - m_f)\, g \tag{38}$$

Revised: August 12, 1993

where m_f is the mass of fluid displaced by the body and $F(t)$ is given by a generalization of (11) for an arbitrary body. The quasi-steady drag is

$$F_{\mathrm{QS}}(t) = -3\pi\mu D V(t)\phi(\mathrm{Re}_D), \tag{39}$$

the history force is generalized to

$$F_H(t) = -3\pi\mu D\int_0^t K(t, s;\mathrm{Re}_D)\dot{V}(s)ds, \tag{40}$$

and the added mass force is given by

$$F_{\mathrm{AM}}(t) = -\kappa m_f\dot{V} \tag{41}$$

where κ depends only on the geometry and takes the value 1/2 for a sphere. In this example F_{FS} is absent since the fluid is at rest.

The terminal velocity, V_T, is determined from

$$V_T\phi_T = \frac{(m-m_f)g}{3\pi\mu D} \tag{42}$$

where $\phi_T = \phi(\mathrm{Re}_T)$ and the terminal Reynolds number is $\mathrm{Re}_T = V_T D/\nu$. We make equation (38) dimensionless using velocity scale V_T and time scale a/V_T, and use v for dimensionless velocity to obtain

$$\phi(\mathrm{Re}_D)v = \phi_T - \beta\dot{v} - \int_0^\tau K(\tau, s;\mathrm{Re}_D)\dot{v}(s)ds \tag{43}$$

with inertia parameter $\beta = (2/3\pi)\,(m+\kappa m_f)\,(V_T/\mu D^2) = (1/9)\,\mathrm{Re}_T\,(m+\kappa m_f)/m_s$, where m_s is the mass of fluid displaced by a spherical body of diameter D.

The result for the force due to a step change in velocity (26) may be generalized to obtain the history force kernel for the case when the particle velocity has been (nearly) constant for a long time after an arbitrary variation:

$$K(\tau, s; \mathrm{Re}_D) \sim 3\mathrm{Re}_T \frac{[\phi(\tau) + \mathrm{Re}_D(\tau)\phi'(\tau)]\,\phi'(s)}{\mathrm{Re}_D(\tau)\left[\int_s^\tau v(s')ds'\right]^2}, \qquad \tau - s \gg 1 \tag{44}$$

When τ is very large, the velocity will have almost reached its terminal value and the history integral may be broken into three parts:

$$I = I_1 + I_2 + I_3 = \int_0^\sigma K(\tau, s; \mathrm{Re}_D)\dot{v}(s)ds + \int_\sigma^{\tau-\sigma} K(\tau, s; \mathrm{Re}_D)\dot{v}(s)ds + \int_{\tau-\sigma}^{\tau} K(\tau, s; \mathrm{Re}_D)\dot{v}(s)ds \tag{45}$$

with $\tau \gg \sigma \gg 1$. The approximate form of the kernel (44) may be used in I_1 and I_2, while the form appropriate to I_3 is not known exactly, but must possess the small-time behavior exhibited in (17).

We assert that for large τ, the velocity defect is algebraically small, $\lambda = 1 - v = O(\tau^{-n})$ with $n > 1$, which may be checked *a posteriori*. Then an order of magnitude analysis indicates that the contribution from I_1 is $O(\tau^{-2})$, from I_2 is $O(\tau^{-2}\sigma^{-n})$ and from I_3 is $O(\tau^{-n-1}\sigma^{1/2})$, so we are left to evaluate I_1:

$$I_1 \sim 3\mathrm{Re}_T \int_0^\sigma \frac{[\phi(\tau) + \mathrm{Re}_D(\tau)\phi'(\tau)]\,\phi'(s)}{\mathrm{Re}_D(\tau)\left[\int_s^\tau v(s')ds'\right]^2}\dot{v}(s)ds \sim 3\left[\frac{\phi(\tau) + \mathrm{Re}_D(\tau)\phi'(\tau)}{\mathrm{Re}_D(\tau)}\right]\frac{\phi(\sigma) - \phi(0)}{\tau^2}. \tag{46}$$

We note that for self-consistency we must take $n = 2$, and that $\dot{v} = O(\tau^{-3})$, so that the direct effects of inertia are negligible. We substitute (46) into (43) to obtain

$$(1-\lambda)\,\phi((1-\lambda)\,\mathrm{Re}_T) \sim \phi_T - \frac{3}{\mathrm{Re}_T}\phi_T[\phi_T + \mathrm{Re}_T\phi'_T]\,\tau^{-2}. \tag{47}$$

Finally, we solve (47) for λ and hence obtain the velocity

$$v \sim 1 - \frac{3}{\mathrm{Re}_T}\phi_T\tau^{-2} \tag{48}$$

We have demonstrated that the approach to terminal velocity of a body in free fall is as the inverse square of time, and this seems to be a universal feature of the long-time behavior for a

Revised: August 12, 1993

body in non-reversing motion. The direct contribution of inertia, $\beta\dot{v}$ in (43), has been neglected in (47), so the final approach to terminal velocity is dictated entirely by the history force and the result is independent of the inertia parameter β. We can use the result (48) directly to find that the inertia term is negligible provided

$$\tau \gg \frac{2\beta}{(\phi_T + \mathrm{Re}_T \phi'_T)} = \frac{2}{9}\left(\frac{m + \kappa m_f}{m_s}\right)\frac{\mathrm{Re}_T}{\phi_T + \mathrm{Re}_T \phi'_T}.$$

For a bubble or a solid particle in a liquid, the density ratio is typically of order unity, so the result (48) is valid for $\tau \gg \mathrm{Re}_T$. For a particle or droplet in gas, however, the density ratio is typically of order 10^3, and (48) will be valid only for extremely long times. This simply means that the history force is not so important in aerosol suspensions. It has been shown by Mei (1993b) for droplets in a gas that even an impulsive acceleration such as may be caused by the passage of a shock wave leads to a negligibly small history force.

5. Discussion

Our principal results are for the long time behavior of the force on a particle due to a change in the free stream velocity from U_1 to U_2. For an impulsively started flow, or a change between two positive speeds, the force approaches the steady value with inverse square decay (26), determined by a simple sink which is generated during the sudden transient and is advected away from the body by the mean flow with velocity U_2. This result is also valid for a non-parallel change in the flow direction, and is almost universally valid. The exceptional cases are an instantaneous reversal of the flow (32) and an impulsively stopped flow (34), for which the force approaches the steady value as τ^{-1} due to the effect of the old wake. The results for the history force may be summarized as:

$$\phi_H \sim \frac{3}{\mathrm{Re}_2}(\phi_2 + \mathrm{Re}_2 \phi'_2)(\phi_2 - \phi_1)\tau^{-2} \qquad U_1 > 0, U_2 > 0$$

$$\phi_H \sim \frac{3}{\mathrm{Re}_2}(\phi_2 + \mathrm{Re}_2 \phi'_2)\phi_2 \tau^{-2} \qquad U_1 = 0, U_2 > 0$$

$$\phi_H \sim \frac{3}{2}(\phi_2 + \mathrm{Re}_2\phi'_2)\frac{\alpha_{12}}{1+\alpha_{12}}\phi_1\tau^{-1} \qquad U_1 < 0, U_2 > 0$$

$$\phi_H \sim \frac{3}{4}\phi_0\phi_1\tau^{-1} \qquad U_1 > 0, U_2 = 0$$

These results are based only on the gross features of the flow in the far field, and so do not depend on the geometry of the body, nor do they require that the near wake should be steady or even laminar (Batchelor 1967). Thus the results are valid for arbitrarily shaped bluff bodies at any Reynolds number with the restriction that $\tau \gg \max\{\mathrm{Re}, \mathrm{Re}^{-1}\}$. However, they are probably most useful for the case of steady laminar wakes in axisymmetric flow with Reynolds number in the range 0.1-100, where the time restriction is not too stringent.

We have also obtained new numerical solutions of the Navier Stokes equations for flow past a sphere with a sudden change in the free stream velocity. The resolution of these calculations is superior to previous work and allows direct comparison with the asymptotic results up to very large times as shown in Figure 3 – Figure 8. The results agree very well with the asymptotic results at large time, and provide a quantitative estimate of the error incurred in applying the asymptotic results at finite time. Calculations for reversed flow and impulsively stopped flow have not been previously reported, and show interesting and unique features. The details of the asymptotic analysis and numerical procedure and the flow fields obtained in the calculations are to be described in a companion paper (Mei & Lawrence 1993).

The low Reynolds number range is of particular interest since rigorous asymptotic results are available for the whole time-history of the force. Results for a solid sphere are shown in Figure 3(a) for $\mathrm{Re} = 0 \rightarrow 0.1$ and in Figure 4(a) for $\mathrm{Re} = 0.1 \rightarrow 0.3$. There is a long time period when the force follows the zero-Reynolds number inverse square root decay of the Basset force, but this ceases at a time of O(1/Re) when the wake extends into the Oseen region, and there is a transition to inverse square decay as predicted above. Sano's (1981) result, and therefore Lovalenti & Brady's (1993a) result, for start-up from rest perform very well in comparison to the numerical solution. However, for a non-zero initial velocity, Lovalenti & Brady's (1993a) result breaks down at large times, due to the dominance of terms of $O(\mathrm{Re}^2)$.

Revised: August 12, 1993

There is a region of "exponential decay", connecting the two algebraic asymptotes, but the long-time inverse square decay is apparent for $\tau > \mathrm{Re}^{-2}$.

We have applied our asymptotic results to the approach to terminal velocity of a body in free fall, and shown that the velocity also decays as the inverse square of time (48). This result is explicitly independent of the inertia parameter β, which may be surprising at first sight. However, at sufficiently long times, the inertia of the particle is smaller than the accumulated inertial effect of the fluid embodied in the history force, so the approach to steady state is governed entirely by the fluid, independent of the particle inertia.

The results presented in this paper are quite simple, but may be of considerable use. Firstly, they serve as a stringent test for the accuracy of time-dependent Navier-Stokes solvers. Indeed, the numerical results presented above were only obtained after we understood the important role played by the moving sink in the wake and sufficiently resolved the flow fields in the new and old wakes and the transition zone. Earlier results (Mei, 1993b) had indicated a decay faster than the inverse square of time, possibly even exponential; this was due to inadequate resolution of the far wake which depletes the strength of the sink. More importantly, the new results provide considerable insight into the mechanisms responsible for the transient force at moderate Reynolds number and may serve as a guide in the construction of approximate formulae for the representation of the transient force on a particle in an arbitrary transient flow. The form proposed by Mei & Adrian (1992) cannot be perfect since it seeks to use a quasi-linear representation to describe a suite of nonlinear problems. However, its qualitative features, in particular the t^{-2} decay of the kernel at long time, are supported by our new results, at least in cases without flow reversal.

As this work was completed, the authors became aware of the Appendix by E. J. Hinch added to Lovalenti & Brady (1993a). The results for impulsively started and stopped flow given above are essentially identical to those given by Hinch.

This work was supported in part by a National Science Foundation award CTS88-57040. CJL is grateful to the faculty of the Department of Mechanical Engineering at the University of Illinois at Chicago for their generous hospitality.

REFERENCES

BASSET, A. B. 1888 *A Treatise on Hydrodynamics*, vol. 2, Dover.

BATCHELOR, G. K. 1967 *An Introduction to Fluid Dynamics*, Cambridge University Press.

CLIFT, R. GRACE, J. R. & WEBER, M. E. 1978 *Bubbles, Drops and Particles*, Academic Press.

HINCH, E. J. 1975 Application of the Langevin equation to fluid suspensions. *J. Fluid Mech.* **72**,499-511.

LAWRENCE, C. J. & WEINBAUM, S. 1988 The unsteady force on a body at low Reynolds number; the axisymmetric motion of a spheroid. *J. Fluid Mech.* **189**, 463-489.

LOVALENTI, P. M. & BRADY J. F. 1993a The hydrodynamic force on a rigid particle undergoing arbitrary time-dependent motion at small Reynolds number. *J. Fluid Mech* in press.

LOVALENTI, P. M. & BRADY J. F. 1993b The unsteady force on a sphere in small amplitude oscillatory motion at finite Reynolds number. *J. Fluid Mech* in press.

LOVALENTI, P. M. & BRADY J. F. 1993c The force on a bubble, drop, or particle in arbitrary time-dependent motion at small Reynolds number. *Phys Fluids A* in press.

MEI, R. 1993a Flow due to an oscillating sphere and an expression for unsteady drag on the sphere at finite Reynolds number. submitted to *J. Fluid Mech.*

MEI, R. 1993b History force on a sphere due to a step change in the free-stream velocity. *Int. J. Multiphase Flow.* **19**(3),509-525

MEI, R. & ADRIAN, R. J. 1992 Flow past a sphere with an oscillation in the free-stream velocity, and unsteady drag at finite Reynolds number. *J. Fluid Mech.* **237**, 323-341.

MEI, R. ADRIAN, R. J. & HANRATTY, T. J. 1991 Particle dispersion in isotropic turbulence under Stokes drag and Basset force with gravitational settling. *J. Fluid Mech.* **225**, 481-495.

MEI, R. & KLAUSNER, J. F. 1992 Unsteady force on a spherical bubble at finite Reynolds number with small fluctuations in the free-stream velocity. *Phys Fluids A* 4(1), 63-70.

MEI, R., KLAUSNER, J. F. & LAWRENCE, C. J. 1993 A note on the history force on a spherical bubble at finite Reynolds number. *Phys Fluids A* in press.

MEI, R. & LAWRENCE, C. J. 1993 The unsteady laminar wake of a bluff body at finite Reynolds number. manuscript in preparation.

MEI, R., LAWRENCE, C. J. & ADRIAN, R. J. 1991 Unsteady drag on a sphere at finite Reynolds number with small fluctuations in the free stream velocity. *J. Fluid Mech.* **233**, 613-628.

POZRIKIDIS, C. 1989 A study of linearized oscillatory flow past particles by the boundary integral method. *J. Fluid Mech.* **202**, 17-41.

REEKS, M. W. & MCKEE, S. 1984 The dispersive effects of Basset history forces on particle motion in turbulent flow. *Phys. Fluids* **27**(7) 1573-1582.

SANO, T. 1981 Unsteady flow past a sphere at low Reynolds number. *J. Fluid Mech.* **112**, 433-441.

WILLIAMS, W. E. 1966 A note on the slow vibrations in a viscous fluid. *J. Fluid Mech.* **25**, 589-590.

Revised: August 12, 1993

FIGURE CAPTIONS

Figure 1 The principal long-range features of the steady flow past a body.

Figure 2 The principal long-range features of the transient flow past a body.

Figure 3 The transient component of the force in impulsively started flow past a sphere ($U_1 = 0$).
(a) $Re_2 = 0.1$, (b) $Re_2 = 1$, (c) $Re_2 = 10$, (d) $Re_2 = 40$.
____ numerical,..... long-time asymptotic, ------ Mei & Adrian (1992),
-.-.-.- small Re (Sano 1981).

Figure 4 The transient component of the force in impulsively changed flow past a sphere ($U_1 > 0$).
(a) $Re_1 = 0.1$, $Re_2 = 0.3$ ($\alpha_{12} = 1/3$).
(b) $Re_1 = 0.8$, $Re_2 = 1.0$ ($\alpha_{12} = 0.8$).
(c) $Re_1 = 10$, $Re_2 = 15$ ($\alpha_{12} = 2/3$).
(d) $Re_1 = 40$, $Re_2 = 60$ ($\alpha_{12} = 2/3$).
(e) $Re_1 = 40$, $Re_2 = 10$ ($\alpha_{12} = 4$).
____ numerical,..... long-time asymptotic, ------ Mei & Adrian (1992),
-.-.-.- small Re, long time (Lovalenti & Brady 1993a).

Figure 5 Variation of the coefficient in $\phi_H = C\tau^{-2}$ with Reynolds number and velocity ratio.
(a) $/C/$, values of α_{12} from top curve to bottom: 0, 4, 0.1, 1.9, 2/3, 4/3, 0.9, 1.1.
(b) $C/(1-\alpha_{12})$, values of α_{12} from top curve to bottom: 0.1, 2/3, 0.9, 1.1, 4/3, 1.9, 4.

Figure 6 The transient part of the drag for reversed flow past a sphere. $Re_1 = 10$, $Re_2 = 10$ ($\alpha_{12} = 1$).
____ numerical,..... long-time asymptotic.

Figure 7 The drag for impulsively stopped flow past a sphere ($U_2 = 0$). $Re_1 = 10$.
____ numerical,..... long-time asymptotic.

Figure 8 The transient component of the force in impulsively started flow past a spherical bubble at $Re_2 = 5$ and 40.

FIGURES

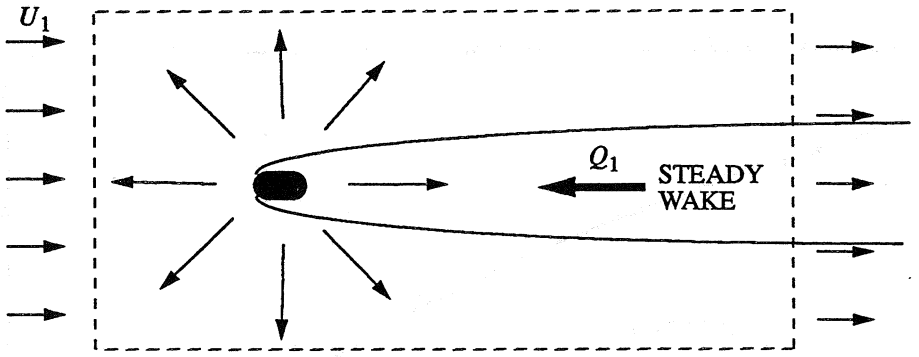

Figure 1 The principal long-range features of the steady flow past a body.

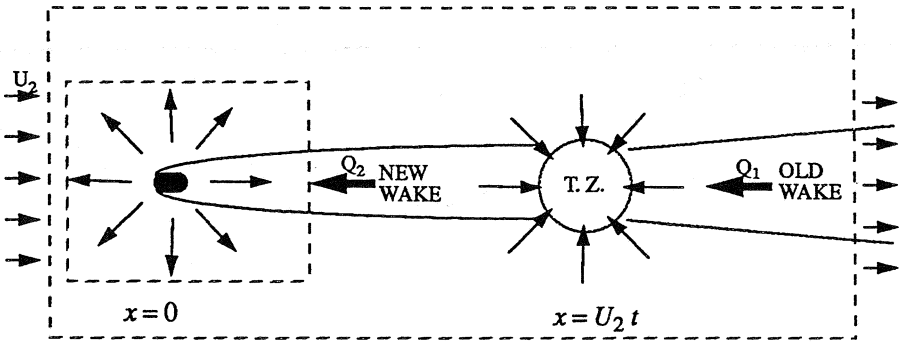

Figure 2 The principal long-range features of the transient flow past a body.

Revised: August 12, 1993

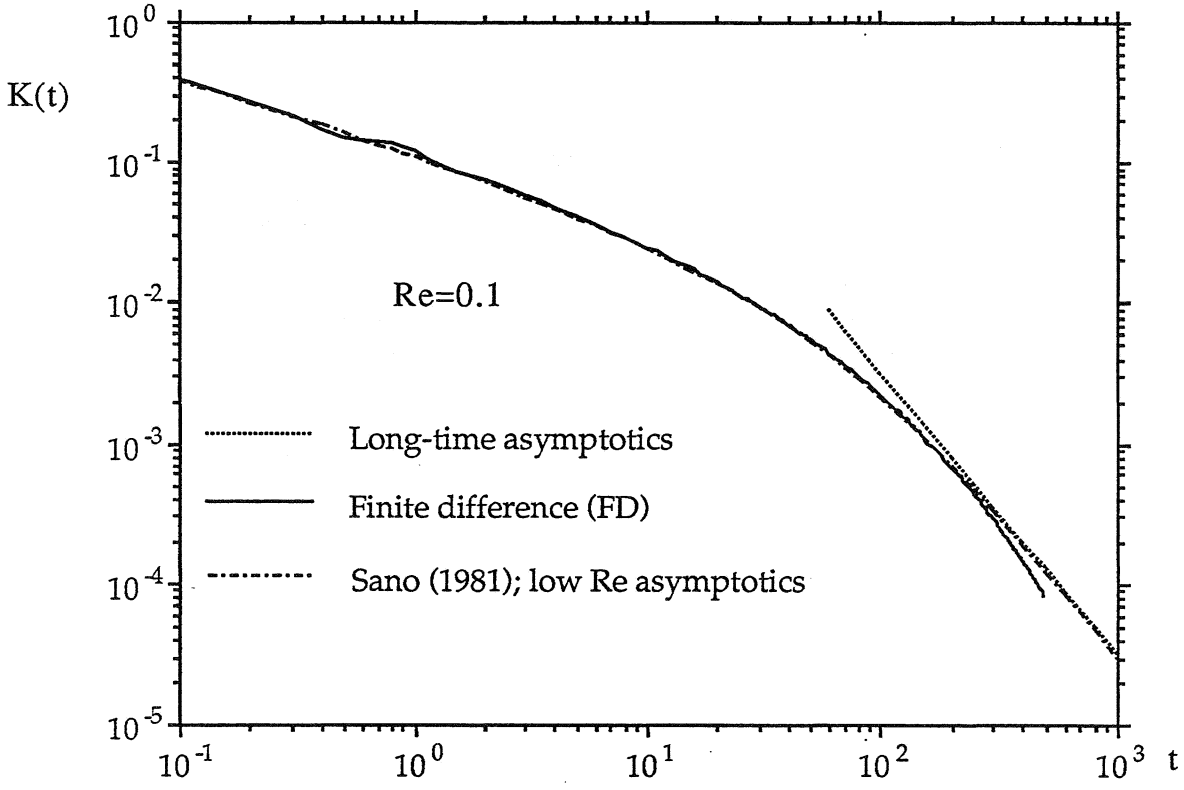
K(t)
10^{0}
10^{-1}
10^{-2}
10^{-3}
10^{-4}
10^{-5}
Re=0.1
Long-time asymptotics
Finite difference (FD)
Sano (1981); low Re asymptotics
10^{-1}
10^{0}
10^{1}
10^{2}
10^{3}
t

Figure 3a

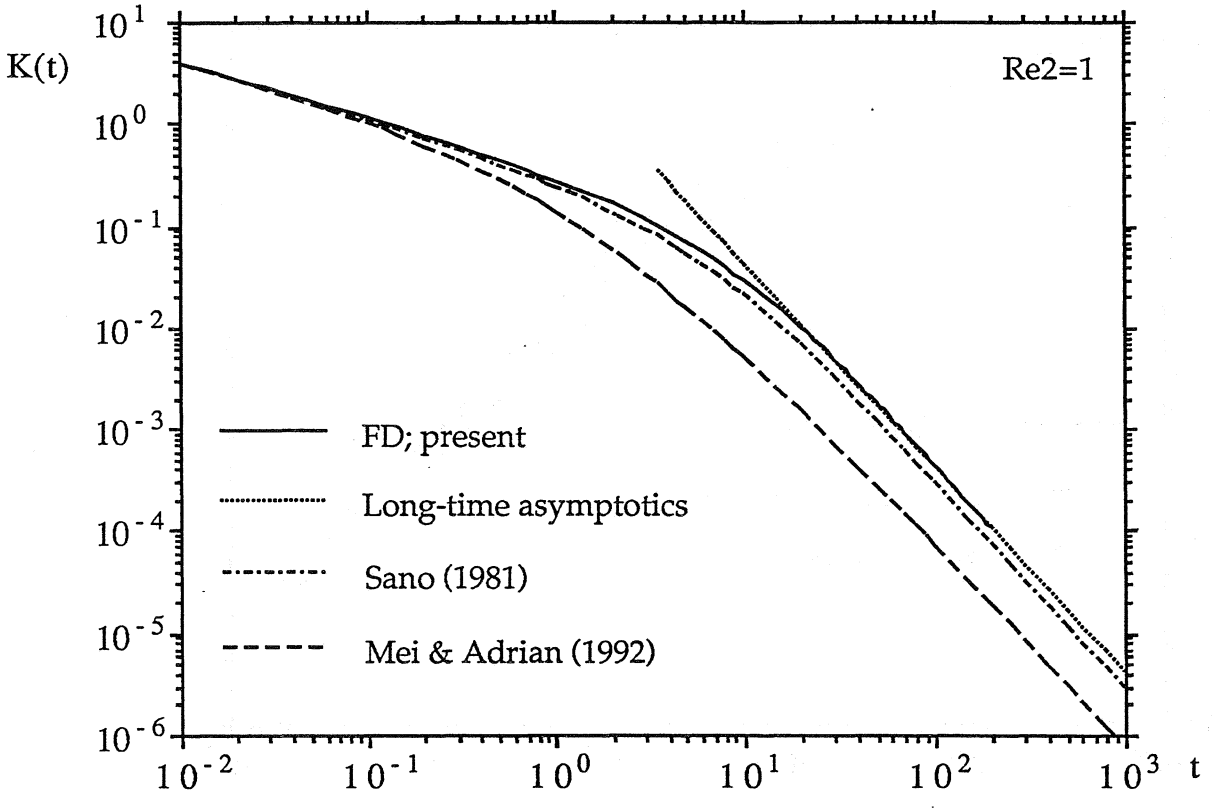
K(t)
Re2=1
FD; present
Long-time asymptotics
Sano (1981)
Mei & Adrian (1992)
t

Figure 3b

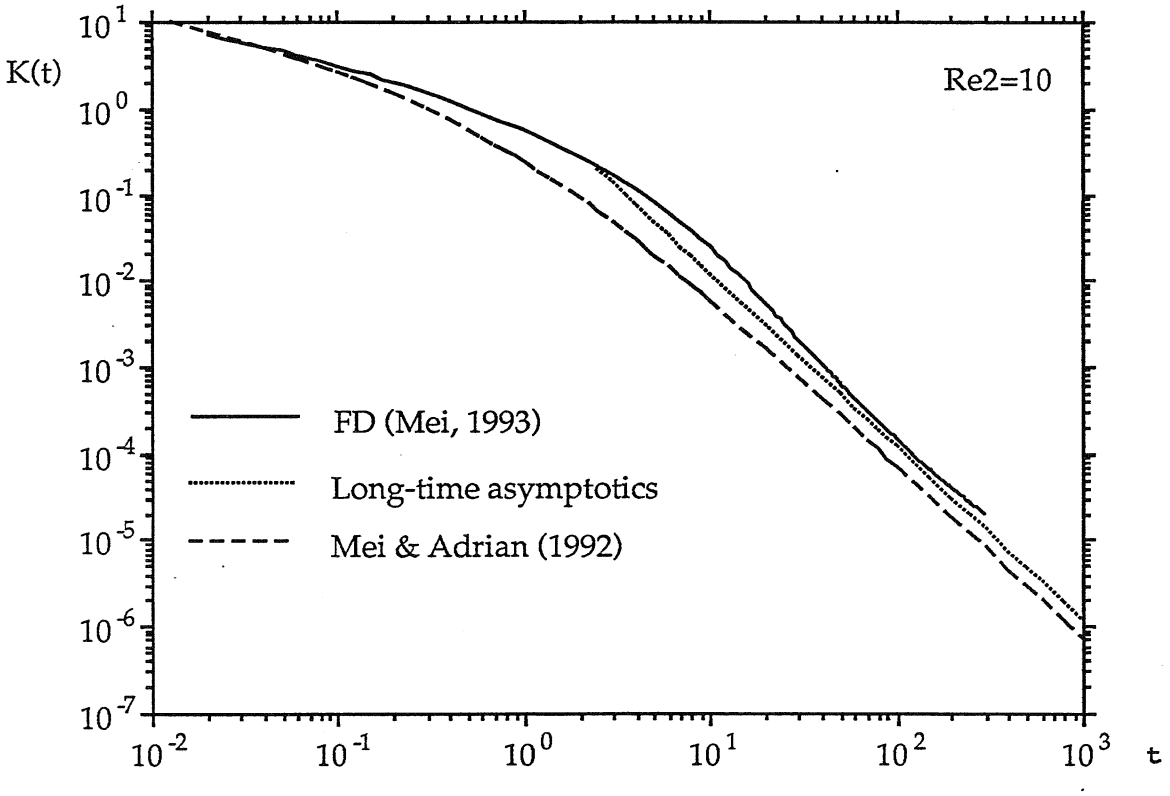

Figure 3c

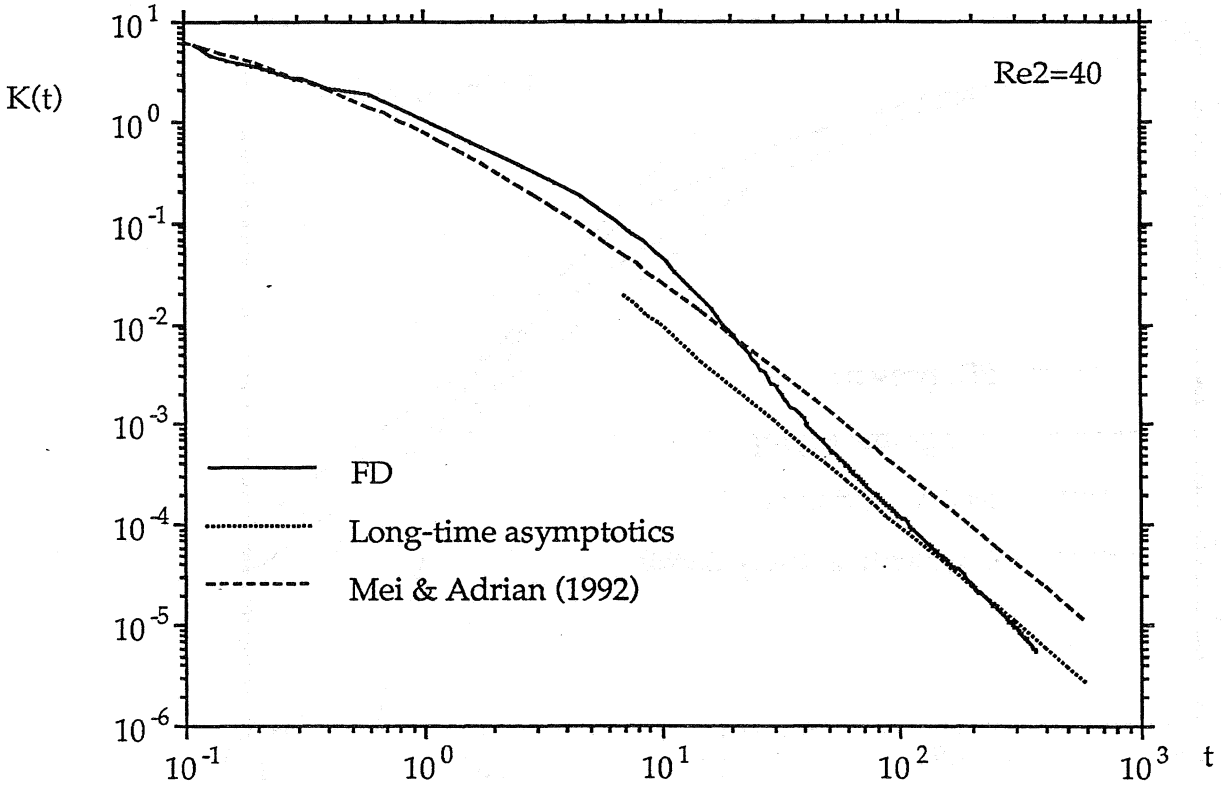

Figure 3d

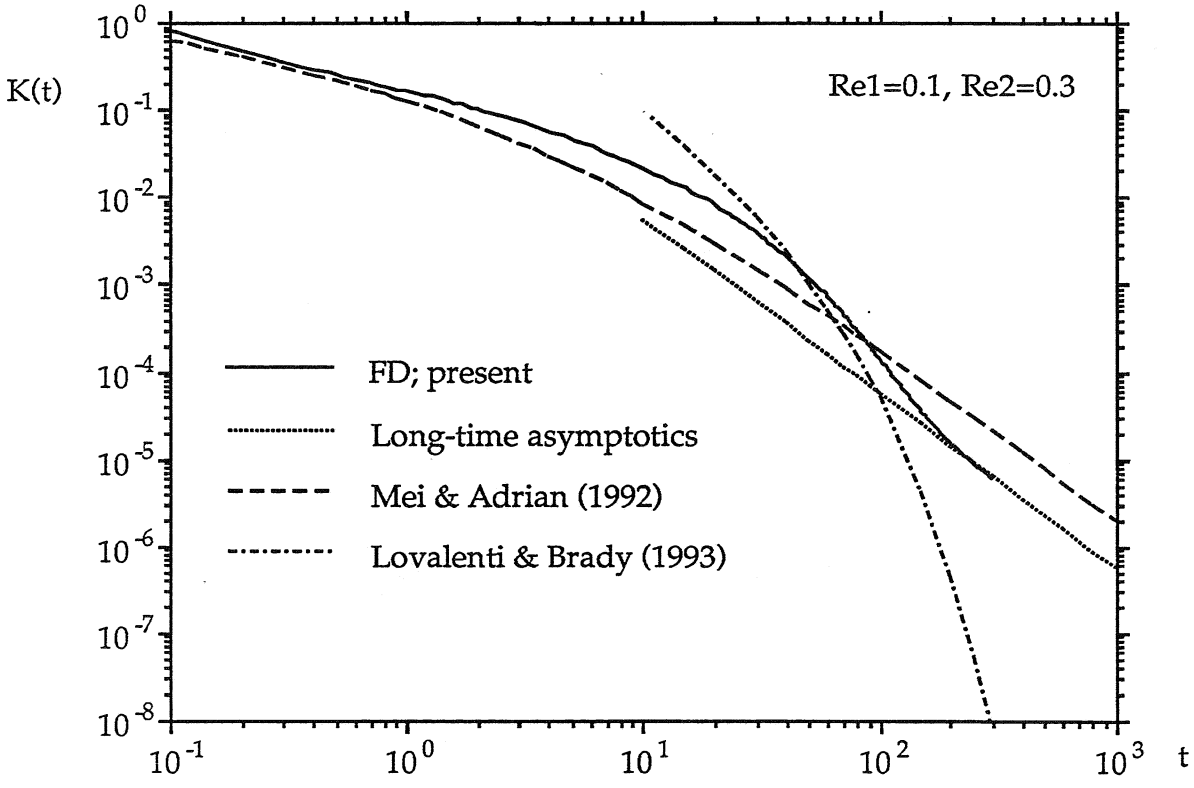
K(t)
Re1=0.1, Re2=0.3
FD; present
Long-time asymptotics
Mei & Adrian (1992)
Lovalenti & Brady (1993)
t

Figure 4a

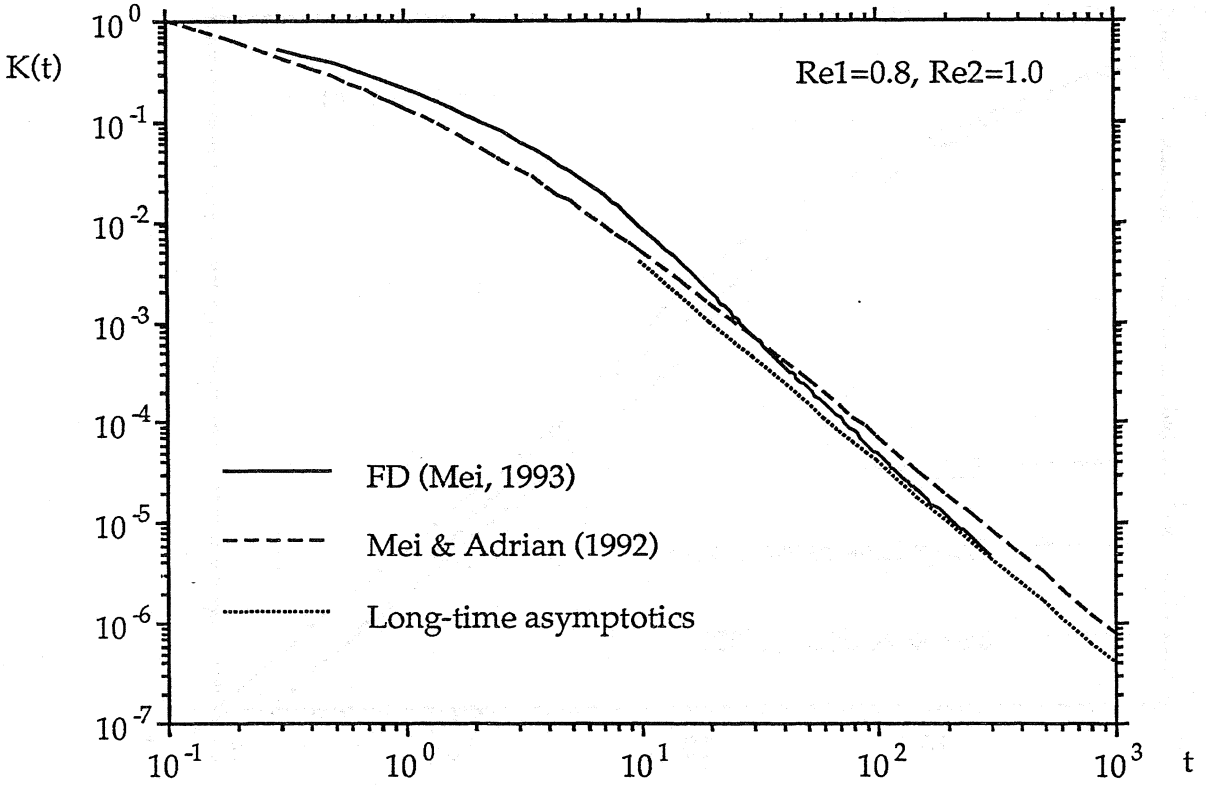
K(t)
Re1=0.8, Re2=1.0
FD (Mei, 1993)
Mei & Adrian (1992)
Long-time asymptotics
t

Figure 4b

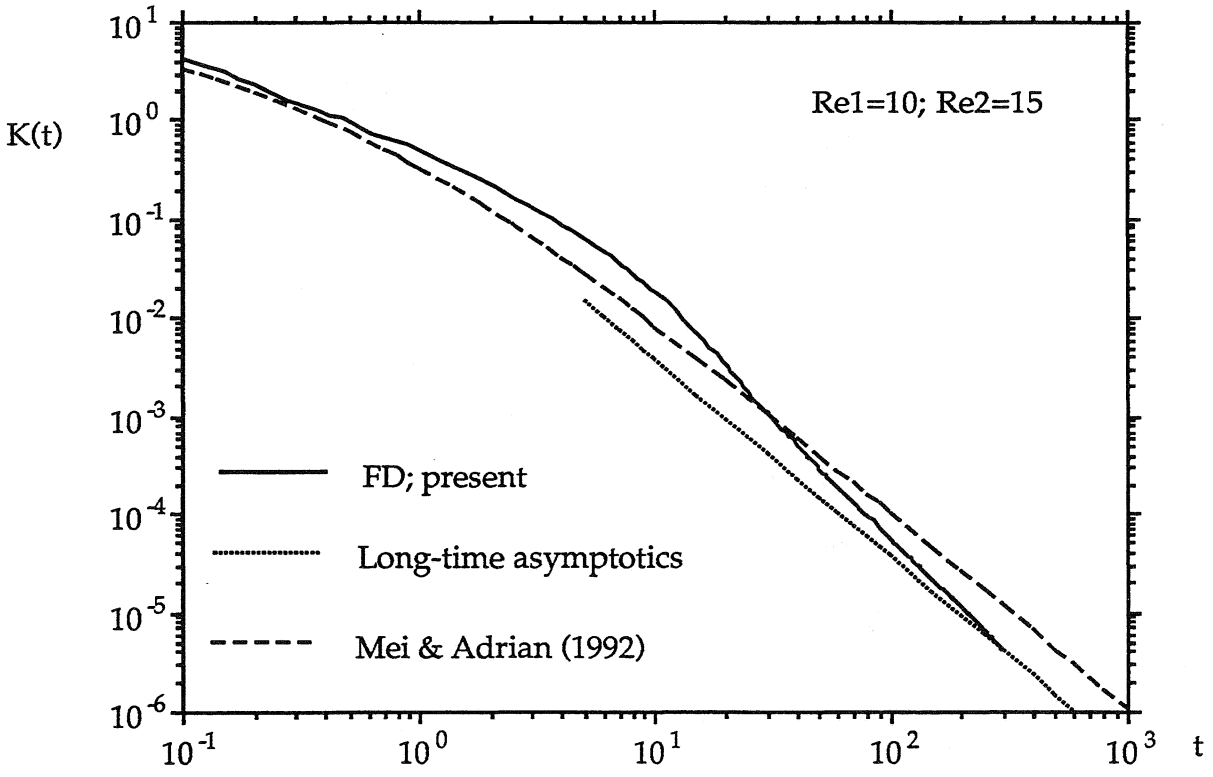
K(t)
10^{1}
10^{0}
10^{-1}
10^{-2}
10^{-3}
10^{-4}
10^{-5}
10^{-6}
Re1=10; Re2=15
FD; present
Long-time asymptotics
Mei & Adrian (1992)
10^{-1}
10^{0}
10^{1}
10^{2}
10^{3}
t

Figure 4c

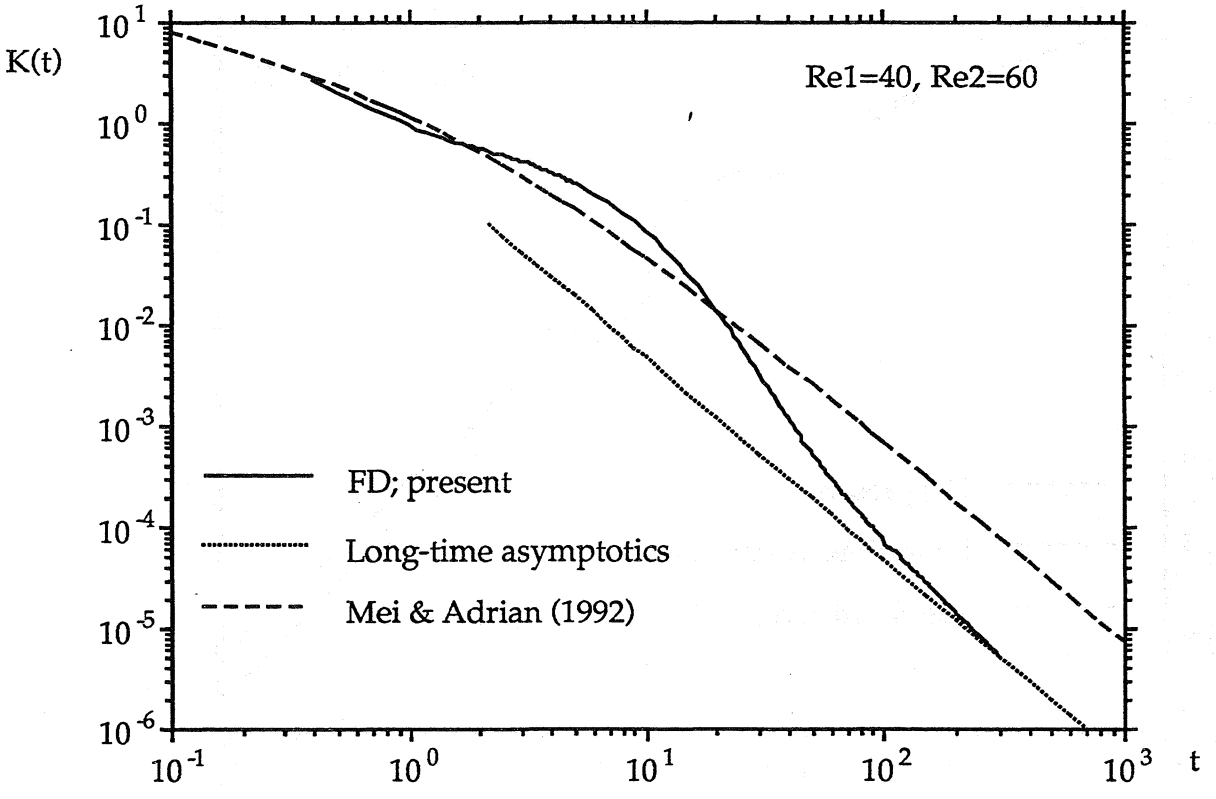
K(t)
Re1=40, Re2=60
FD; present
Long-time asymptotics
Mei & Adrian (1992)
t

Figure 4d

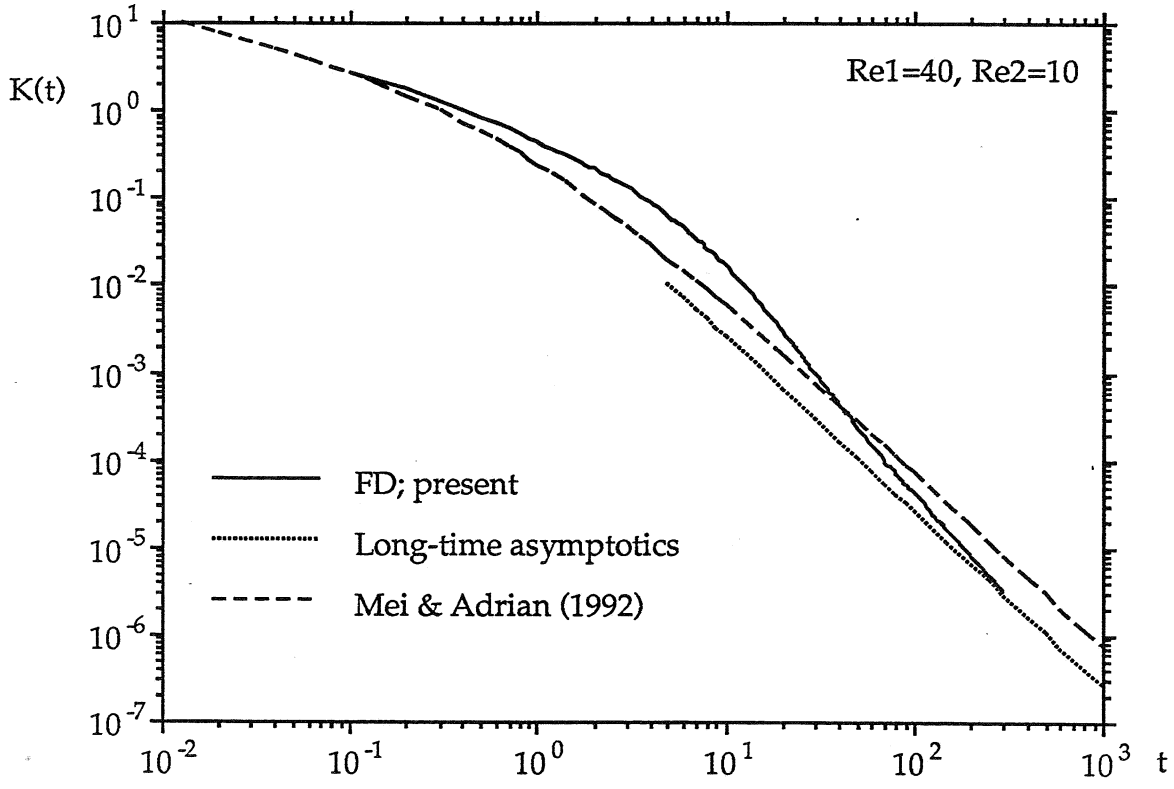
K(t)
Re1=40, Re2=10
FD; present
Long-time asymptotics
Mei & Adrian (1992)
t

Figure 4e

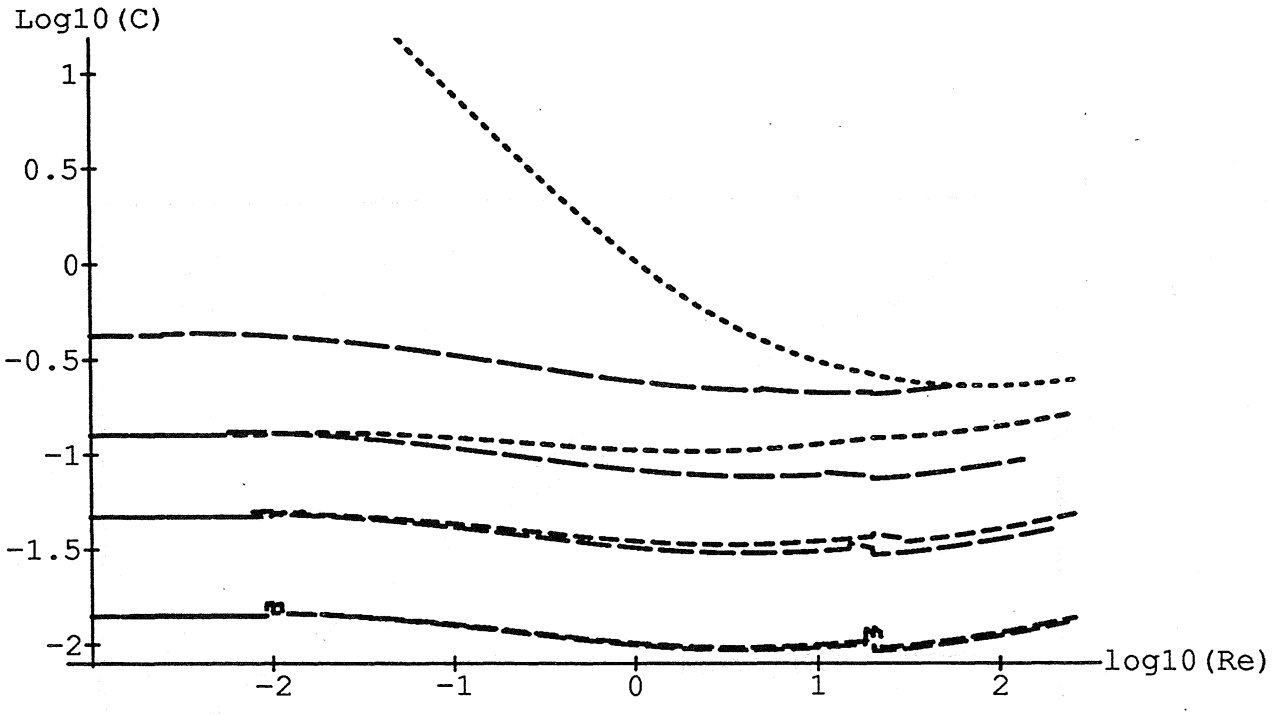

Figure 5a

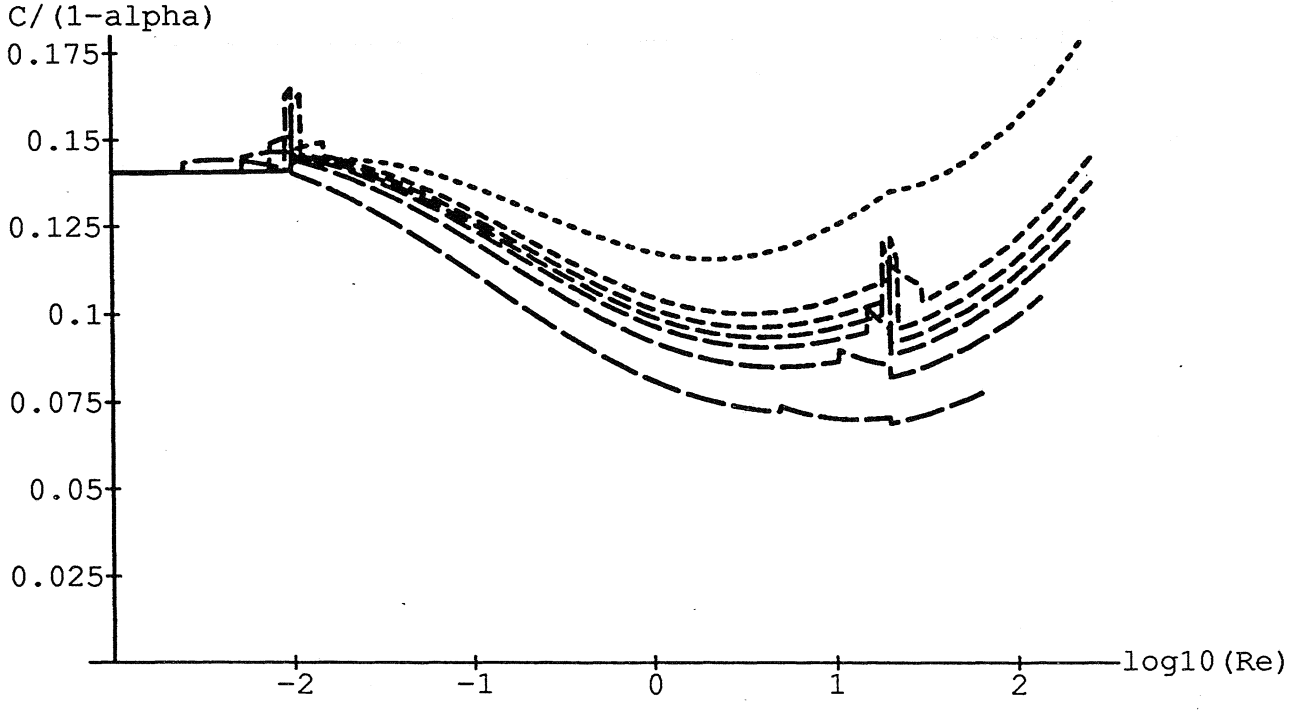

Figure 5b

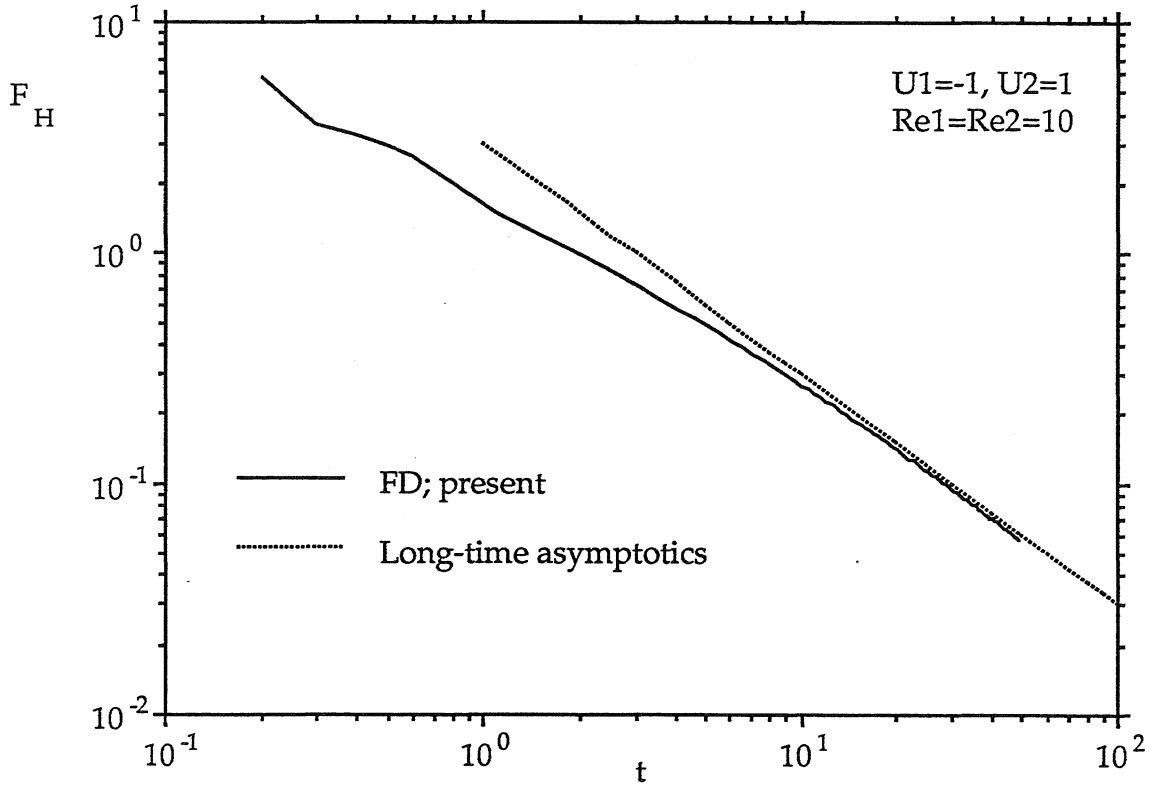
10^1
10^0
10^{-1}
10^{-2}
F_H
U1=-1, U2=1
Re1=Re2=10
FD; present
Long-time asymptotics
10^{-1}
10^0
10^1
10^2
t

Figure 6

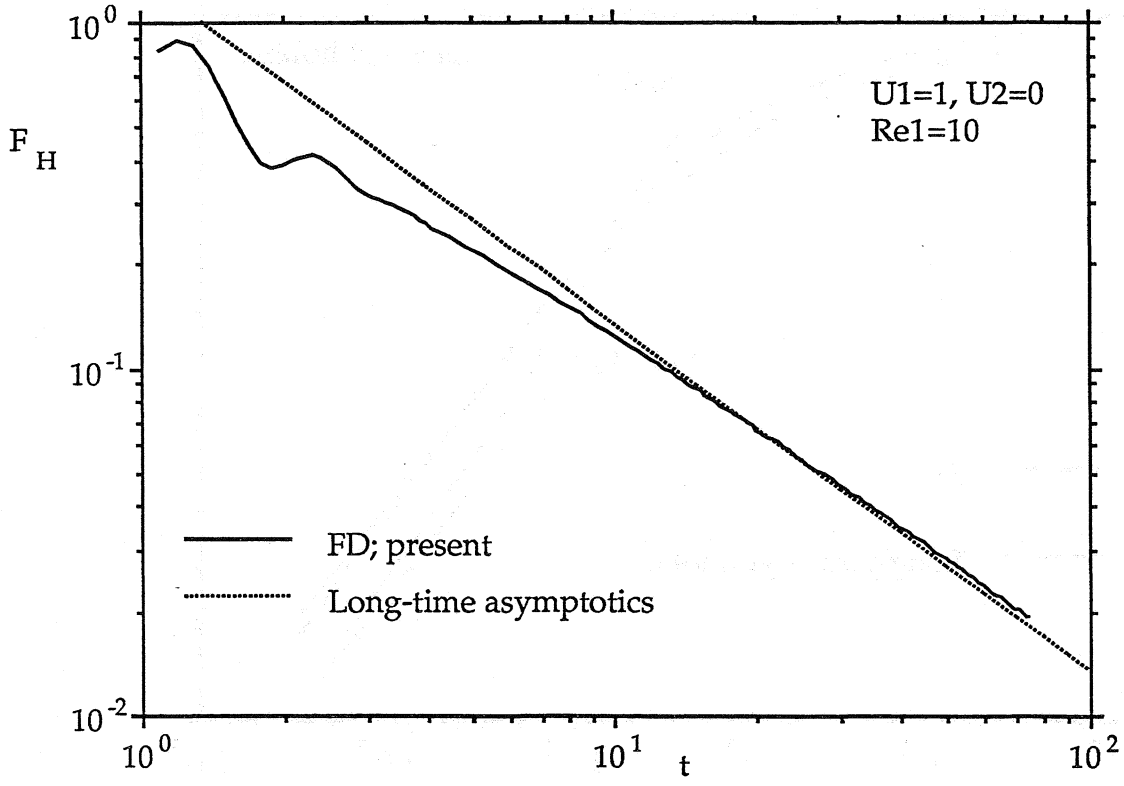
10^0
10^{-1}
10^{-2}
F_H
U1=1, U2=0
Re1=10
FD; present
Long-time asymptotics
10^0
10^1
t
10^2

Figure 7

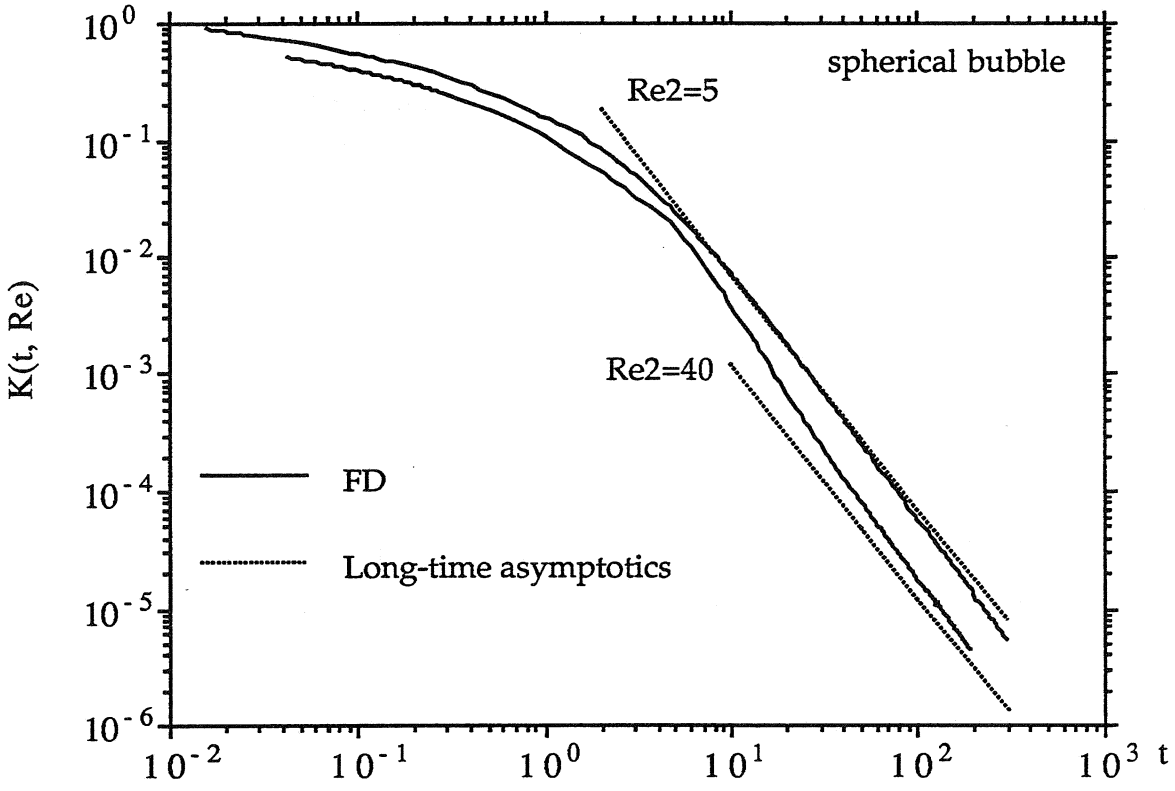
spherical bubble
Re2=5
Re2=40
FD
Long-time asymptotics
K(t, Re)
t
10^{0}
10^{-1}
10^{-2}
10^{-3}
10^{-4}
10^{-5}
10^{-6}
10^{-2}
10^{-1}
10^{0}
10^{1}
10^{2}
10^{3}

Figure 8

List of Recent TAM Reports

No.	Authors	Title	Date
497	Powers, J. M., and D. S. Stewart	Approximate solutions for oblique detonations in the hypersonic limit	Apr. 1991
498	Davidson, M. T., K. L. Kuster, K. W. Quinn, N. A. Sluz, and G. Stojkovich	Twenty-fifth student symposium on engineering mechanics, M. E. Clark, coord. (1988)	Feb. 1992
499	Cardenas, H. E., W. C. Crone, D. J. Scott, G. G. Stewart, and B. F. Tatting	Twenty-sixth student symposium on engineering mechanics, M. E. Clark, coord. (1989)	Mar. 1992
700	Juister, C. E., D. W. Newport, C. S. Payne, J. M. Peters, M. P. Thomas, and J. C. Trovillion	Twenty-seventh student symposium on engineering mechanics, M. E. Clark, coord. (1990)	Apr. 1992
701	Bernard, R. T., D. W. Claxon, J. A. Jones, V. R. Nitzsche, and M. T. Stadtherr	Twenty-eighth student symposium on engineering mechanics, M. E. Clark, coord. (1991)	Apr. 1992
702	Greening, L. E., P. J. Joyce, S. G. Martensen, M. D. Morley, J. M. Ockers, M. D. Taylor, and P. J. Walsh	Twenty-ninth student symposium on engineering mechanics, J. W. Phillips, coord. (1992)	May 1992
703	Kuah, H. T., and D. N. Riahi	Instabilities and transition to chaos in plane wakes	Nov. 1992
704	Stewart, D. S., K. Prasad, and B. W. Asay	Simplified modeling of transition to detonation in porous energetic materials	Nov. 1992
705	Stewart, D. S., and J. B. Bdzil	Asymptotics and multi-scale simulation in a numerical combustion laboratory	Jan. 1993
706	Hsia, K. J., Y.-B. Xin, and L. Lin	Numerical simulation of semi-crystalline Nylon 6: Elastic constants of crystalline and amorphous parts	Jan. 1993
707	Hsia, K. J., and J. Q. Huang	Curvature effects on compressive failure strength of long fiber composite laminates	Jan. 1993
708	Jog, C. S., R. B. Haber, and M. P. Bendsoe	Topology design with optimized, self-adaptive materials	Mar. 1993
709	Barkey, M. E., D. F. Socie, and K. J. Hsia	A yield surface approach to the estimation of notch strains for proportional and nonproportional cyclic loading	Apr. 1993
710	Feldsien, T. M., A. D. Friend, G. S. Gehner, T. D. McCoy, K. V. Remmert, D. L. Riedl, P. L. Scheiberle, and J. W. Wu	Thirtieth student symposium on engineering mechanics, J. W. Phillips, coord. (1993)	Apr. 1993
711	Weaver, R. L.	Anderson localization in the time domain: Numerical studies of waves in two-dimensional disordered media	Apr. 1993
712	Cherukuri, H. P., and T. G. Shawki	An energy-based localization theory: Part I—Basic framework	Apr. 1993
713	Manring, N. D., and R. E. Johnson	Modeling a variable-displacement pump	June 1993
714	Birnbaum, H. K., and P. Sofronis	Hydrogen-enhanced localized plasticity—A mechanism for hydrogen-related fracture	July 1993
715	Balachandar, S., and M. R. Malik	Inviscid instability of streamwise corner flow	July 1993
716	Sofronis, P.	Linearized hydrogen elasticity	July 1993
717	Nitzsche, V. R., and K. J. Hsia	Modelling of dislocation mobility controlled brittle-to-ductile transition	July 1993
718	Hsia, K. J., and A. S. Argon	Experimental study of the mechanisms of brittle-to-ductile transition of cleavage fracture in silicon single crystals	July 1993
719	Cherukuri, H. P., and T. G. Shawki	An energy-based localization theory: Part II—Effects of the diffusion, inertia and dissipation numbers	Aug. 1993
720	Aref, H., and S. W. Jones	Chaotic motion of a solid through ideal fluid	Aug. 1993
721	Stewart, D. S.	Lectures on detonation physics: Introduction to the theory of detonation shock dynamics	Aug. 1993
722	Lawrence, C. J., and R. Mei	Long-time behavior of the drag on a body in impulsive motion	Sep. 1993